

Outliers of Dust Along the Southern Margin of the Tharsis Region, Mars

J. R. Zimbelman

Center for Earth and Planetary Studies, National Air and Space Museum,
Smithsonian Institution, Washington, DC 20560

This work documents the distinctive characteristics of two locations near the southeastern margin of the Tharsis low thermal inertia region on Mars that support the inferred south-to-north migration of dust deposits under present climatic conditions (Christensen, 1986, 1988). Low thermal inertia and high albedo indicate the presence of fine-grained surface materials on the highly fractured terrain of northern Claritas Fossae (-16° , 110°), with a narrow zone of fine material connecting this location to the southern margin of the Tharsis low thermal inertia region. A similar deposit occurs in Sinai Planum (-16° , 80°) on an isolated exposure of fractured terrain. In comparison to their surroundings, both locations have higher visual albedo, lower thermal inertia, and higher topographic relief coupled with lower reflectivity and higher roughness at radar wavelengths. The Sinai Planum location has less contrast with its surroundings at all wavelengths than the Claritas Fossae location. The remote-sensing data are interpreted to indicate erosional stripping of dust deposits that progressed in a northerly direction, with dust preferentially preserved on rough surfaces due to reduced efficiency of aeolian erosion.

INTRODUCTION

Global mapping of the thermal properties of Mars identified three continent-scale regions of low thermal inertia, interpreted to consist of very fine (silt-sized) particles at the surface (Kieffer *et al.*, 1977; Zimbelman and Kieffer, 1979; Palluconi and Kieffer, 1981). Recent synthesis of global properties at visual, thermal, and radar wavelengths led to the hypothesis that the low thermal inertia regions consist of dust deposits, on the order of meters in thickness, that are redistributed around the planet as changing insolation conditions alter the global wind regime (Christensen, 1986). Variations in the pattern of atmospheric clearing following global dust storms indicate a net south-to-north transport of dust under present climatic conditions (Christensen, 1988). However, the lack of large, identifiable dust deposits in the southern hemisphere at present makes it difficult to relate the dust transportation to the evolution of the regional dust deposits. In this paper the distinctive characteristics of two locations near the southeastern margin of the Tharsis low thermal inertia region are documented and are shown to support the inferred south-to-north migration of dust deposits under present climatic conditions.

BACKGROUND

The Tharsis and Elysium volcanic provinces and cratered highlands in the Arabia region all have distinctive remote-sensing characteristics. Comparison of the physical properties in these three regions provide consistent results of low thermal inertia, high visual albedo, and considerable roughness at radar wavelengths, interpreted to result from the penetration of the radar signal through a comparatively thin dust mantle with subsequent scattering by roughness elements on the underlying volcanic and cratered terrains (Christensen, 1986). Imaging observations of wind streaks and variable features indicate that significant sediment transport within the Tharsis

region occurred during the Viking mission, with downslope winds carrying materials away from the Tharsis shield volcanoes (Lee *et al.*, 1982). However, changes in the overall distribution of the large regional dust deposits are likely driven by changes in climate and global circulation (Christensen, 1986, 1988).

It seems unlikely that the migration of the dust deposits can be observed directly, due to the long timescales (ranging from tens of thousands to millions of years) thought to be associated

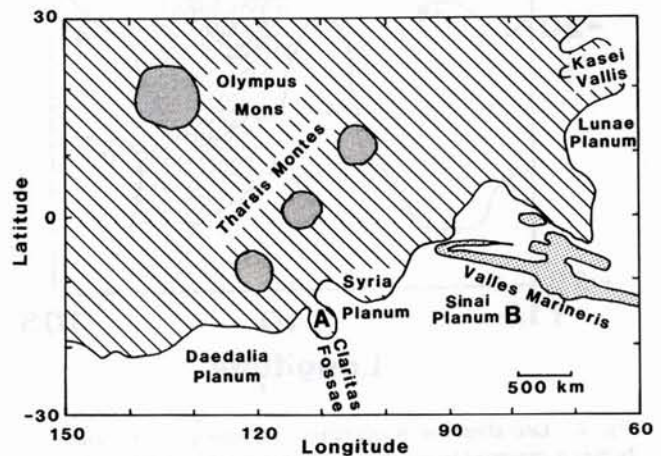


Fig. 1. Location map for the Claritas Fossae (A) and Sinai Planum (B) features described in the text. The large shield volcanoes of Tharsis (dark pattern) and Valles Marineris (stippled pattern) are shown for reference, as well as the names of several prominent features. The lined pattern indicates the extent of the Tharsis low thermal inertia region within the map area. The boundary of the Tharsis region corresponds to the -10 K contour (equivalent to a thermal inertia of about 4×10^{-3} cal cm^{-2} $\text{sec}^{-1/2}$ K^{-1}) of the predawn residual temperature maps of Kieffer *et al.* (1977) and Zimbelman and Kieffer (1979).

with climatic changes on Mars (e.g., *Ward, 1974*). This conclusion is consistent with thermal measurements made throughout the Viking mission that failed to detect evidence of a change in the position of the margins of the three low thermal inertia regions (*Zimbelman and Kieffer, 1979*), implying that the present margins of the dust deposits are stable on a scale of tens of kilometers. Even if the migration

of the dust deposits cannot be observed directly, there may be remnants of a former dust mantle that could indicate the general direction in which the dust deposits have moved under recent climatic conditions. The approach adopted here is to look for evidence of a previous dust mantle that can be related to the present dust deposits.

The largest of the three regional dust deposits surrounds the Tharsis Montes extending over 130° of longitude and 60° of latitude and encompassing an area of 22 million km^2 , only slightly smaller than the area of the North American continent (*Zimbelman and Kieffer, 1979*). The southern margin of the Tharsis region skirts the northern edge of the Valles Marineris canyon system and follows an irregular course across Sinai, Syria, and Daedalia Planae (Fig. 1). The eastern margin includes a pronounced embayment into the low thermal inertia material along Kasei Vallis, the site of considerable aeolian activity and abundant sand-sized material confined within the channel (*Christensen and Kieffer, 1979*). The south-to-north transport of dust observed under present climatic conditions (*Christensen, 1988*) implies that evidence for previous dust deposits should exist along the southern margin of the deposit.

Claritas Fossae is a complex assemblage of grabens and fractured terrain associated with a projection of low thermal inertia material into the higher thermal inertia materials of the southern hemisphere (A in Fig. 1). The distinctive thermal properties of Claritas Fossae were first noted early in the Viking mission (*Kieffer et al., 1976*; see Fig. 2), but this area received less attention than did the unusual thermal characteristics on and around Arsia Mons. During an examination of the published physical properties of Claritas Fossae, a second location of fractured terrain in Sinai Planum (B in Fig. 1) was observed to have many characteristics similar to Claritas Fossae but generally with less contrast in comparison to its surroundings (*Zimbelman, 1989*). Both locations have bedrock interpreted to be highly deformed, fractured materials of Noachian age, the oldest of the martian stratigraphic systems (*Scott and Tanaka, 1986*). Many additional outcrops of this old, fractured terrain are present in the cratered highlands south of the Valles Marineris (*Scott and Tanaka, 1986*), but only the two locations described above have remote-sensing characteristics comparable to those of the regional dust deposits. The variations in the remotely observed properties of the ancient, fractured materials provide strong clues to the direction in which a migrating dust mantle could have moved across Mars.

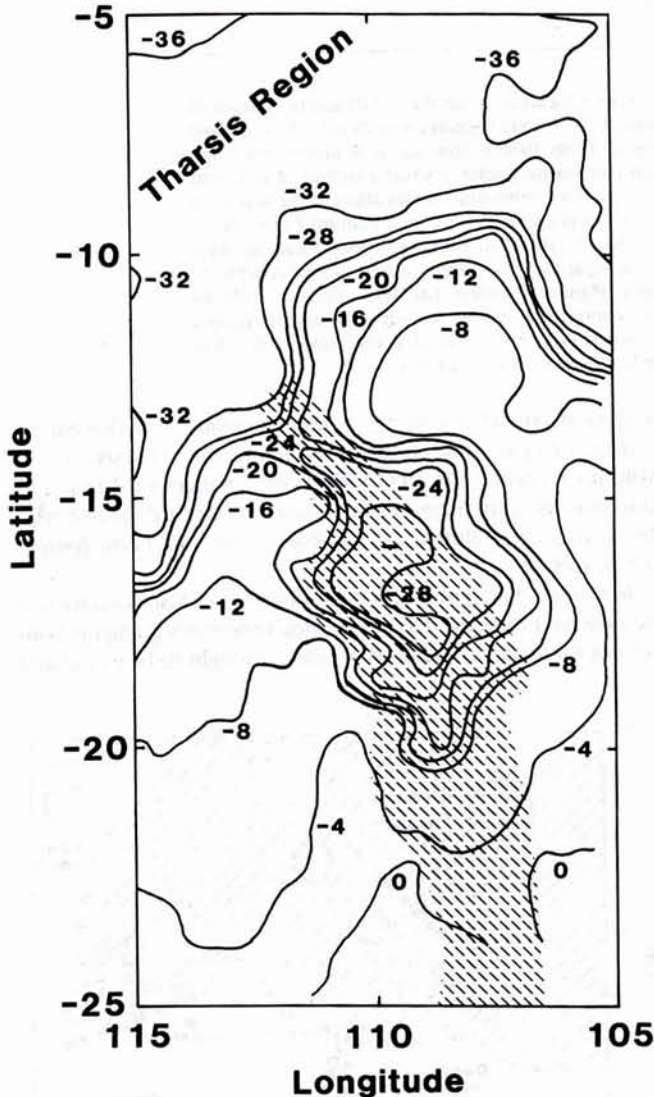


Fig. 2. Late afternoon temperature residuals (the difference between observed temperature and that predicted for a Mars average thermal inertia of $6.5 \times 10^{-3} \text{ cal cm}^{-2} \text{ sec}^{-1/2} \text{ K}^{-1}$ and albedo of 0.25) for Claritas Fossae (modified from Fig. 4B of *Kieffer et al., 1976*). Dashed pattern indicates the extent of ancient, fractured terrain (from *Scott and Tanaka, 1986*). Temperature residuals of -28 K , -8 K , and 0 K are equivalent to thermal inertias of 2.5, 4.5, and $6.5 \times 10^{-3} \text{ cal cm}^{-2} \text{ sec}^{-1/2} \text{ K}^{-1}$, respectively. The low temperature residuals (low thermal inertia) on Claritas Fossae are concentrated north of -20° lat., and they are comparable to the temperature residuals within the nearby Tharsis region.

DATA

The physical properties of both the Claritas Fossae and Sinai Planum locations of ancient, fractured terrain are summarized below. All of the data have been published previously, but here the results for Claritas Fossae and Sinai Planum are examined within the context of the proposed global transport of dust on Mars.

Thermal Inertia

The northern portion of Claritas Fossae (Fig. 2) has temperature residuals indicative of a thermal inertia much lower ($I < 3$) than its immediate surroundings ($I > 5$). A zone



Fig. 3. Northern portion of Claritas Fossae. The area of low thermal inertia corresponds to the high albedo material visible here (compare with Fig. 2). The lowest thermal inertias occur on the highly fractured terrain (-16° lat., 110° long.) below the center of the scene shown here. Portion of Viking Orbiter frame 334S12 (centered on -14° lat., 110° long.), red filter, 790 m/pixel, shading corrected rectilinear version.

of low thermal inertia material connects the Tharsis region with the low thermal inertia material on the northern portion of Claritas Fossae, centered approximately on -16° lat., 110° long. The thermal properties of northern Claritas Fossae are comparable to the properties of the large regions of low thermal inertia, interpreted to be a surface mantled by silt-size material (Kieffer *et al.*, 1977). It is significant that the fractured terrain of Claritas Fossae south of -20° lat. has thermal properties very similar to the moderate thermal inertias typical of the southern midlatitudes of Mars, in great contrast to the distinctive thermal properties of northern Claritas Fossae.

Fractured terrain in Sinai Planum (centered approximately on -16° lat., 80° long.) also has temperature residuals indicative of a thermal inertia lower than its surroundings, although the thermal contrast is considerably reduced compared to that of northern Claritas Fossae. Global mapping of predawn temperature residuals (Fig. 9b of Kieffer *et al.*, 1977) shows the Sinai Planum location to be between 0 and 2 K ($I = 6.5$), while the surrounding plains have temperature residuals between 4 and 6 K ($I = 7.5$). Such a small thermal contrast might seem insignificant if it did not also correlate with distinct properties at both visual and radar wavelengths.

Visual Albedo

Subtle albedo variations in the vicinity of Valles Marineris are portrayed dramatically in a recent color mosaic (McEwen, 1987). Northern Claritas Fossae has a higher albedo than its

surroundings, particularly at red wavelengths (Fig. 3). It is not a coincidence that the planimetric shape of the high albedo region on northern Claritas Fossae corresponds to the general shape of the low thermal inertia material at this same location (compare Figs. 2 and 3). Global mapping has revealed a planetwide correlation between low thermal inertia and high visual albedo (Kieffer *et al.*, 1977; Arvidson *et al.*, 1982), a relationship that holds down to a scale of a few kilometers, the highest resolution of the Viking Infrared Thermal Mapper data (Zimbelman and Lesbin, 1987). Results for northern Claritas Fossae are very consistent with this well-documented global trend. South of -20° lat. Claritas Fossae lacks a prominent albedo contrast with its surroundings, consistent with the reduced contrast of this area at thermal wavelengths.

The Sinai Planum location has a slightly higher albedo on the southern portion of the fractured terrain (Fig. 4), coincident with the area that shows the subtle thermal contrast. As was the case at thermal wavelengths, the high albedo portion of the Sinai Planum location has considerably less contrast with its surroundings at visual wavelengths than does northern Claritas Fossae. The reduced contrast does not keep this location from being visible in the color mosaic (McEwen, 1987).

Radar Topography and Surface Roughness

Both the northern Claritas Fossae and the Sinai Planum dust deposits are located on terrain possessing considerable

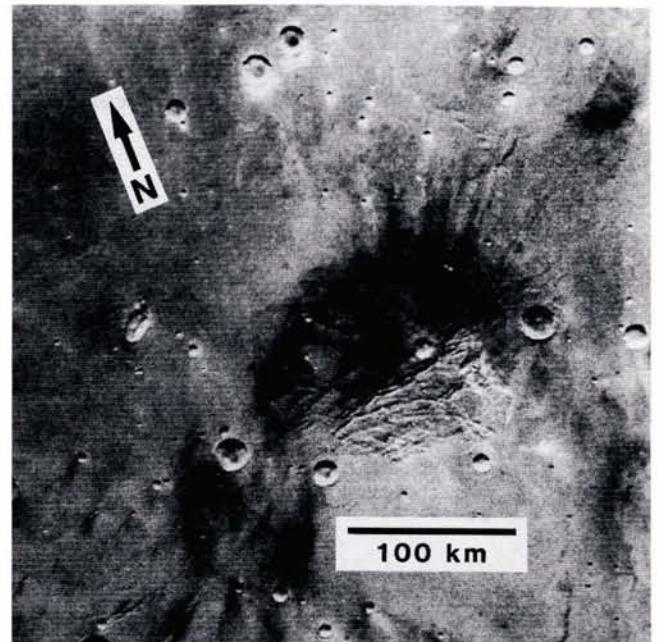


Fig. 4. Fractured terrain in Sinai Planum. The high albedo material on the southern portion of the fractured terrain has physical properties similar to the northern portion of Claritas Fossae (see Fig. 3), but the Sinai Planum location generally has less contrast with its surroundings than does the Claritas Fossae location. Portion of Viking Orbiter frame 334S46 (centered on -15° lat., 80° long.), red filter, 790 m/pixel, shading corrected rectilinear version.

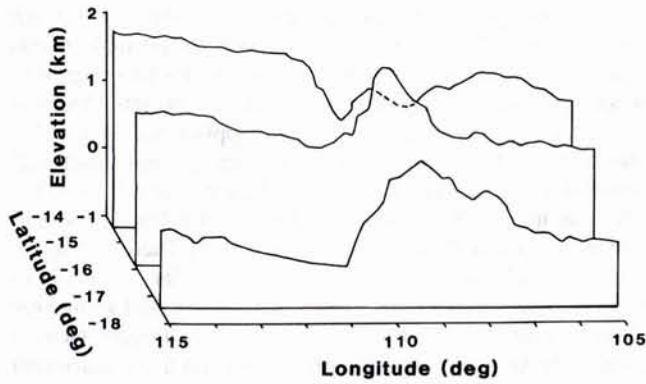


Fig. 5. Topographic profiles across northern Claritas Fossae obtained from Earth-based radar measurements (modified from Fig. 7 of Roth *et al.*, 1980). The dust deposit is associated with the prominent ridge possessing relief on the order of one kilometer, in contrast to the more subdued plains on either side. Dashed line shows the portion of a profile hidden by an intervening profile in this particular projection. The base of each profile is plotted at the latitude of the corresponding groundtrack (from north to south these latitudes are -14.50° , -15.91° , and -17.46°). Profiles are shown at $100\times$ vertical exaggeration.

topographic relief. Earth-based radar measurements indicate that northern Claritas Fossae consists of a broad ridge that stands more than one kilometer above the uniform plains on either side of the ridge (Fig. 5). The topographic ridge corresponds closely with the location of the dust deposit inferred from the visual and thermal measurements. Similarly, the fractured terrain in Sinai Planum also possesses relief

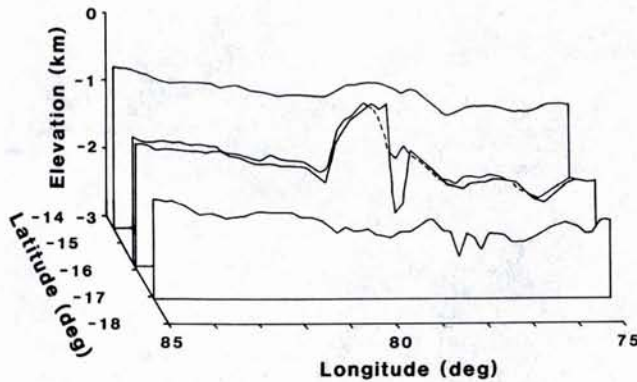


Fig. 6. Topographic profiles across the Sinai Planum fractured terrain obtained from Earth-based radar measurements (modified from Fig. 8 of Roth *et al.*, 1980). As is the case with Claritas Fossae (see Fig. 5), the dust deposit is associated with relief on the order of one kilometer, in contrast to the more subdued plains on either side. Dashed line shows the portion of a profile hidden by an intervening profile in this particular projection. The base of each profile is plotted at the latitude of the corresponding groundtrack (from north to south these latitudes are -14.50° , -15.80° , -15.91° , and -17.08°). Profiles are shown at $100\times$ vertical exaggeration.

greater than one kilometer, again in contrast to the relatively flat plains surrounding the topographic high (Fig. 6). The area of greatest relief within the fractured terrain of Sinai Planum occurs at a latitude of -16° , precisely where the dust deposit is inferred from the other remote sensing data.

Radar measurements also provide information on the scattering characteristics of the martian surface on a scale comparable to or larger than the radar wavelength (12 cm for the data described below). Northern Claritas Fossae and the fractured terrain in Sinai Planum both stand out from their surroundings in several parameters obtained from the characteristics of the reflected radar signal (Fig. 7). Both locations have low reflectivity and high roughness and RMS slopes, relative to the surrounding terrain, but the contrast is

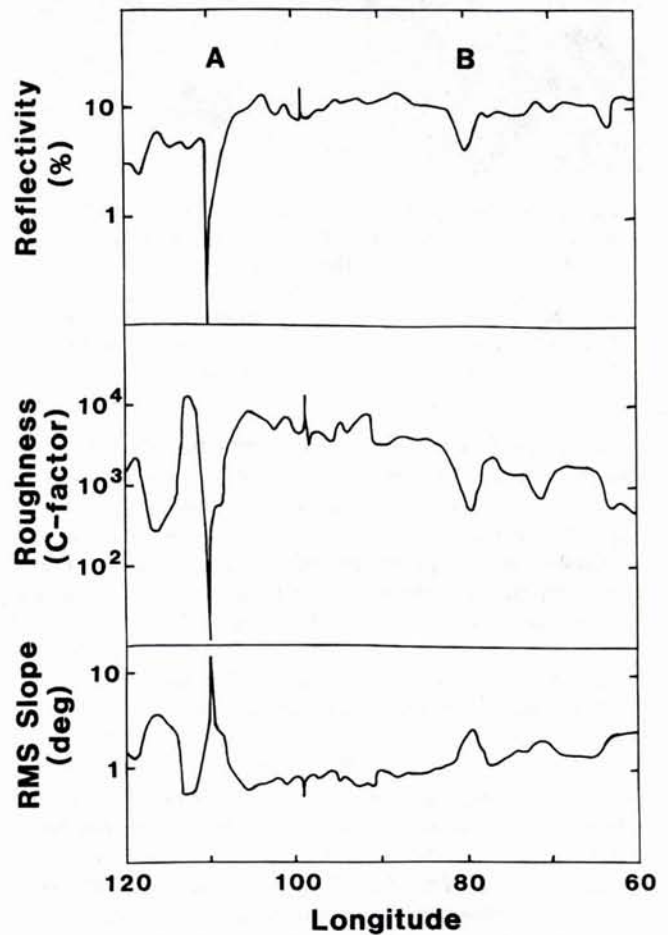


Fig. 7. Surface properties obtained from Earth-based radar measurements (modified from Fig. 7 of Downs *et al.*, 1975). The data are for a latitude of -16° , where A and B indicate the locations of fractured terrain in northern Claritas Fossae and Sinai Planum, respectively. Note that the C-factor (center diagram) is smaller for rough surfaces than for smooth surfaces. Both locations have decreased reflectivity and increased roughness and RMS slope, relative to their surroundings, but the magnitude of the contrast is much greater at northern Claritas Fossae than at Sinai Planum.

much more pronounced at Claritas Fossae than at Sinai Planum. The RMS slope values are particularly instructive; Claritas Fossae has a maximum RMS slope greater than 10° at long. 110° , while Sinai Planum has a fairly uniform RMS slope of 3° , and both locations are surrounded by plains with slopes of 1° or less (Fig. 7). These distinctive radar properties are unique within the longitude range of 0° to 120° , at a latitude of -16° , except for Valles Marineris and Arsia Mons.

Enhanced roughness and/or decreased reflectivity in the Tharsis region correlate well with lava flows that are observed to have a relatively thin aeolian mantle when examined in Viking images with a resolution of 15 m/pixel or better (Schaber, 1980). Although images of this resolution do not exist for the areas of Claritas Fossae and Sinai Planum under discussion here, it seems reasonable to conclude that the radar data are sensing a rough, irregular surface (on a scale of 1 to 100 m) that do not contribute to the remote-sensing characteristics at visual and thermal wavelengths.

DISCUSSION

All of the remote-sensing data for northern Claritas Fossae and the fractured terrain in Sinai Planum are consistent with a surface that is rough and irregular at the meter scale but that is mantled by fine dust that dominates the surface properties at the centimeter (and smaller) scale. This is precisely the surface condition inferred by Christensen (1986) to characterize the large, low thermal inertia dust deposits of the northern midlatitudes. Of equal importance is the fact that several other nearby locations of ancient, fractured materials do not have anomalous remote-sensing properties, but rather these features have properties quite similar to their surroundings. The fractured terrains having characteristics of dust deposits are at a latitude comparable to the current southern margin of the nearby Tharsis dust deposit (see Fig. 1), while the fractured terrain locations lacking evidence of a dust covering are south of -20° lat., strengthening the likelihood of a causal relationship between the large and small dust deposits.

The requirement that the surface properties be dominated by dust at thermal wavelengths implies an average dust thickness of at least several centimeters, while the penetration of the dust by the radar signals, to the underlying rough surface, implies an average dust thickness that is probably not much greater than a few meters (Christensen, 1986). A similar analysis procedure indicates that northern Claritas Fossae has a dust deposit comparable to the large regional dust deposits, while the fractured terrain at Sinai Planum probably has a dust cover on the order of centimeters thick, still sufficient to affect visual albedo and the diurnal variation of surface temperatures but thin enough to cause reduced contrast between the dust deposit and the surrounding plains.

How did this nonuniform distribution of dust on isolated areas of rough terrain come about? It is possible that the dominance of roughness on the fractured terrain may be so strong that subsequent aeolian erosion may be unimportant. If surface roughness is the primary agent responsible for producing dust deposits, then one should expect to find dust

trapped on all of the numerous outcrops of fractured terrain mapped south of -20° lat. between 70° and 110° long. (Scott and Tanaka, 1986). The lack of anomalous remote sensing properties for Nectaris Fossae (fractured terrain between -18° and -25° lat. along long. 58°) indicates that the lack of preserved dust deposits on fractured terrains is not solely due to latitude but also is related to increased distance from the present margins of the Tharsis dust deposit. These factors make it highly unlikely that roughness alone can explain the isolated dust deposits.

Is there evidence that the isolated dust deposits are the result of aeolian activity? The available image resolution is not sufficient to provide diagnostic evidence for the process of deposit formation, but temporal variations provide an important clue. Images from both Mariner 9 and Viking show considerable variation in the occurrence and orientation of bright streaks in Syria Planum just north of the dust deposit on northern Claritas Fossae (Thomas and Veverka, 1979). These same images show virtually no change in the high albedo material on northern Claritas Fossae. Also, streak orientations indicate winds capable of moving surface materials are blowing toward the north on the western side of Claritas Fossae, while winds blow to the south on the eastern side of Claritas Fossae (Thomas and Veverka, 1979). Thus, there is evidence of considerable aeolian activity in the vicinity of Claritas Fossae and the nonuniform wind direction may contribute to the relative stability of surface materials on Claritas Fossae itself. It seems reasonable to infer an aeolian origin for the dust deposit on northern Claritas Fossae and, by analogy, for the thinner dust deposit in Sinai Planum.

Why are the dust deposits located on rough terrain? Field studies, laboratory simulations, and theoretical considerations indicate that increased roughness at the surface increases the difficulty of moving material by the wind by decreasing the wind shear at the particulate surface (Bagnold, 1941, pp. 53-55). It is important to realize that surface roughness can vary both on small (less than one meter) and large (greater than many meters) scales where small-scale roughness can protect erodible elements, such as dust, while large-scale roughness tends to enhance wind shear and the possibility of erosion (Lee et al., 1982). It is the small-scale roughness that affects the wind shear at the surface and creates an aerodynamic regime in which mobile particles (dust or sand) are protected from the lifting forces of the wind. There is no reason to expect dust to be preferentially deposited on the rough terrains on Mars, but once on the surface it is more difficult to remove the dust from rough terrains without reducing the local roughness.

Are there isolated dust deposits near the southern margins of the other regional dust deposits on Mars? There do not appear to be isolated deposits elsewhere along the southern margin of the Tharsis region nor along the southern margins of the Elysium or Arabia regions. This result may be partly due to the lack of isolated regions with properties as distinctive as those observed at northern Claritas Fossae, but it may also be related to the lack of exposures of ancient, fractured terrain near the southern margins of the regional dust deposits except at the locations discussed here. Isolated deposits smaller than

about 25 km probably are present, but these deposits likely will be detectable only with the highest resolution data.

The interpretations described here do not provide conclusive verification of the migration of regional dust deposits on Mars, but the spatial relationship and the local contrast of the remote-sensing properties at northern Claritas Fossae and Sinai Planum provide some compelling circumstantial evidence for the regional migration. Erosional removal of a previously widely distributed dust deposit seems the simplest explanation for the occurrence of isolated dust deposits on rough terrain near the margin of a regional dust deposit, while other exposures of similar rough terrain do not display evidence of the dust deposit. Alternative mechanisms can be proposed for isolated dust accumulations, but it seems unlikely that a nonaeolian process would be as consistent with the spatial distribution and the observed remote-sensing characteristics. Since Sinai Planum is both further removed from the present margin of the Tharsis dust deposit (see Fig. 1) and has less dust preserved than at northern Claritas Fossae, the inferred removal of the hypothesized dust mantle should have progressed from south to north, as inferred from the hypothesis of *Christensen* (1986).

CONCLUSIONS

Remote-sensing characteristics at visual, thermal, and radar wavelengths are used to infer the presence of isolated dust deposits on areas of fractured terrain in northern Claritas Fossae and Sinai Planum. The dust deposit at Sinai Planum is probably less thick than the deposit at northern Claritas Fossae, which is comparable to the dust present within the nearby Tharsis low thermal inertia region. Numerous exposures of fractured terrain are present in this area south of -20° lat. but these locations lack distinctive contrast with their surroundings in the remote-sensing data. Aeolian removal of a previously widely distributed dust deposit is interpreted to be the most likely explanation for the isolated dust deposits that have been preserved because they exist on rough terrain that decreases the local efficiency of aeolian erosion. The different distances of the Claritas Fossae and Sinai Planum dust deposits from the southern margin of the Tharsis low thermal inertia region, in combination with a thinner dust deposit at Sinai Planum, indicate that the removal of a widely distributed dust deposit progressed from the south to the north, in agreement with the global movement of dust proposed by *Christensen* (1986).

Acknowledgments. The comments of S. Lee, S. Williams, and an anonymous reviewer were very helpful during the revision of the manuscript. This work was supported by NASA grant NAGW-1390.

REFERENCES

- Arvidson R. E., Guinness E. A., and Zent A. P. (1982) Classification of surface units in the equatorial region of Mars based on Viking Orbiter color, albedo, and thermal data. *J. Geophys. Res.*, *87*, 10149-10157.
- Bagnold R. A. (1941) *The Physics of Blown Sand and Desert Dunes*. Chapman and Hall, London. 265 pp.
- Christensen P. R. (1986) Regional dust deposits on Mars: Physical properties, age, and history. *J. Geophys. Res.*, *91*, 3533-3545.
- Christensen P. R. (1988) Global albedo variations on Mars: Implications for active aeolian transport, deposition, and erosion. *J. Geophys. Res.*, *93*, 7611-7624.
- Christensen P. R. and Kieffer H. H. (1979) Moderate resolution thermal mapping of Mars: The channel terrain around the Chryse basin. *J. Geophys. Res.*, *84*, 8233-8238.
- Downs G. S., Reichley P. E., and Green R. R. (1975) Radar measurements of martian topography and surface properties: The 1971 and 1973 oppositions. *Icarus*, *26*, 273-312.
- Kieffer H. H., Christensen P. R., Martin T. Z., Miner E. D., and Palluconi F. D. (1976) Temperatures of the martian surface and atmosphere: Viking observation of diurnal and geometric variations. *Science*, *194*, 1346-1351.
- Kieffer H. H., Martin T. Z., Peterfreund A. R., Jakosky B. M., Miner E. D., and Palluconi F. D. (1977) Thermal and albedo mapping of Mars during the Viking primary mission. *J. Geophys. Res.*, *82*, 4249-4292.
- Lee S. W., Thomas P. C., and Veverka J. (1982) Wind streaks in Tharsis and Elysium: Implications for sediment transport by slope winds. *J. Geophys. Res.*, *87*, 10,025-10,041.
- McEwen A. S. (1987) Mars as a planet (abstract). In *Lunar and Planetary Science XVIII*, pp. 612-613. Lunar and Planetary Institute, Houston.
- Palluconi F. D. and Kieffer H. H. (1981) Thermal inertia mapping of Mars from 60° S to 60° N. *Icarus*, *45*, 415-426.
- Roth L. E., Downs G. S., Saunders R. S., and Schubert G. (1980) Radar altimetry of south Tharsis, Mars. *Icarus*, *42*, 287-316.
- Schaber G. G. (1980) Radar, visual and thermal characteristics of Mars: Rough planar surfaces. *Icarus*, *42*, 159-184.
- Scott D. H. and Tanaka K. L. (1986) Geologic map of the western equatorial region of Mars. *U.S. Geol. Surv. Map I-1802-A*.
- Thomas P. and Veverka J. (1979) Seasonal and secular variation of wind streaks on Mars: An analysis of Mariner 9 and Viking data. *J. Geophys. Res.*, *84*, 8131-8146.
- Ward W. R. (1974) Climatic variations on Mars. 1. Astronomical theory of insolation. *J. Geophys. Res.*, *79*, 3375-3386.
- Zimbelman J. R. (1989) Erosional outliers of dust along the southern margin of the Tharsis region, Mars (abstract). In *Lunar and Planetary Science XX*, pp. 1237-1238. Lunar and Planetary Institute, Houston.
- Zimbelman J. R. and Kieffer H. H. (1979) Thermal mapping of the northern equatorial and temperate latitudes of Mars. *J. Geophys. Res.*, *84*, 8239-8251.
- Zimbelman J. R. and Leshin L. A. (1987) A geologic evaluation of thermal properties for the Elysium and Aeolis quadrangles of Mars. *Proc. Lunar Planet. Sci. Conf. 17th*, in *J. Geophys. Res.*, *92*, E588-E586.